Sources of plasma in the high altitude cusp

W.K. Peterson, Laboratory for Atmospheric and Space Physics, Boulder, Colorado, USA.
K.J. Trattner, [1]Lockheed-Martin Advanced Technology Center, Palo Alto, California, USA

Submitted to the *Journal of Atmospheric and Solar Terrestrial Physics*, January 2011
Revised, May, 2011

Abstract:

Ambiguities introduced by the inconsistent definitions of the low and high altitude cusp lead to the inconsistency that at low altitudes the region commonly known as the cusp does not include boundary layer plasmas, but at high altitudes it does. Here we examine plasma data from two high altitude cusp intervals where ~100 keV ionospheric ions were observed. We show that the data are an average over an interval that includes plasma from both boundary layer and newly injected solar wind plasmas. We find that the ~100 keV ionospheric ions reported in the high altitude cusp are energized by well known magnetospheric processes bringing energetic ions to the dayside boundary layers. We conclude that there is no need to postulate new processes associated with waves in diamagnetic cavities commonly found in the high altitude cusp to explain the observation of ~100 keV ionospheric ions found there.

Keywords: high altitude cusp, energetic ions, plasma energization

Introduction:

The confusion about what exactly is the cusp has been a recurring theme in magnetospheric physics. The magnetospheric cusp was first identified in the ionosphere by its very large signal in magnetometer, electron, and ion sensors. At low altitudes the cusp is generally identified as a spatially compact magnetospheric region associated with intense fluxes of low energy (~ 100 eV) precipitating solar wind electrons and ions reaching down to the upper regions of Earth's ionosphere (e.g. Meng and Candidi, 1985). We now know that the most intense solar wind fluxes come directly from reconnection sites (e.g., Cowley, 1990, Gosling et al., 1990, Fuselier et al., 1991, Lavraud et al., 2005a Trattner et al., 2010). Differences in the cusp signature and the sensitivities of the various instruments used to identify the low altitude cusp in the 70's and 80's lead to confusion about how extensive in local time the cusp actually was. At an international conference on the cusp Heikkila (1985) summarized the initial observations and observed:

> *"Solar wind plasma comes down the cusp to low altitudes; the remarkably broad area over which this penetration occurs prompted the use of the term cleft, apparently at the foot of the entry layer inside the magnetopause. The consensus of the discussion at the workshop was that cusp should refer mainly to the narrow region defined by the solar wind plasma (perhaps somewhat modified by acceleration or retardation processes); distinctive feature observable in the ionosphere or on the ground are photo-emission, electromagnetic waves, and turbulence."*

The term cleft in the quote above has fallen out of use as our understanding of magnetospheric boundary layers has evolved. As higher sensitive plasma instruments returned data from the dayside magnetosphere, low latitude boundary layer, magnetopause, mantle, and magnetosheath it became possible to distinguish newly injected solar wind plasma from that in adjacent regions where the relatively cold solar wind plasma has been heated and mixed with hot magnetospheric plasma. For a review of boundary layer plasmas see Hultqvist et al., 1999 and references therein. A recent review of the cusps may be found in Cargill et al. (2005). Newell and Meng (1988, 1989) demonstrated a quantitative difference between ion energy spectra in the low altitude cusp and adjacent boundary layers. Newell and his colleagues have demonstrated that it is possible to consistently define magnetospheric regions based on large-scale statistical databases of plasma and field observations at ionospheric altitudes. In their case they have used thermal plasma (i.e. less than 1keV) measurements from Defense Meteorological Satellite Program (DMSP) satellites (circular polar orbit at 800 km altitude) and the fact that ions from regions of newly reconnected solar wind plasma have their maximum fluxes at lower energies than in other regions to define quite precisely what the cusp is at that altitude. Figure 1 reproduced from Newell et al. (2004) shows a clear distinction between cusp, boundary layer, and other magnetospheric regions adjacent to the cusp based on peak energy and number flux of the precipitating ions and electrons. The data shown in Figure 1 are averages obtained from 11 years of DMSP data during intervals when the interplanetary magnetic field (IMF) Bz and By components were both positive. It is important to note that the cusp identified in Figure 1 is a region of newly injected solar

wind plasma. Figure 1 also shows a region called the mantle poleward of the cusp and boundary layers that can contain solar wind plasmas on older open field lines. Mantel and boundary layer plasmas are usually warmer than cusp plasma (Newell et al., 2004) and generally include larger magnetospheric populations depending on the direction of the IMF.

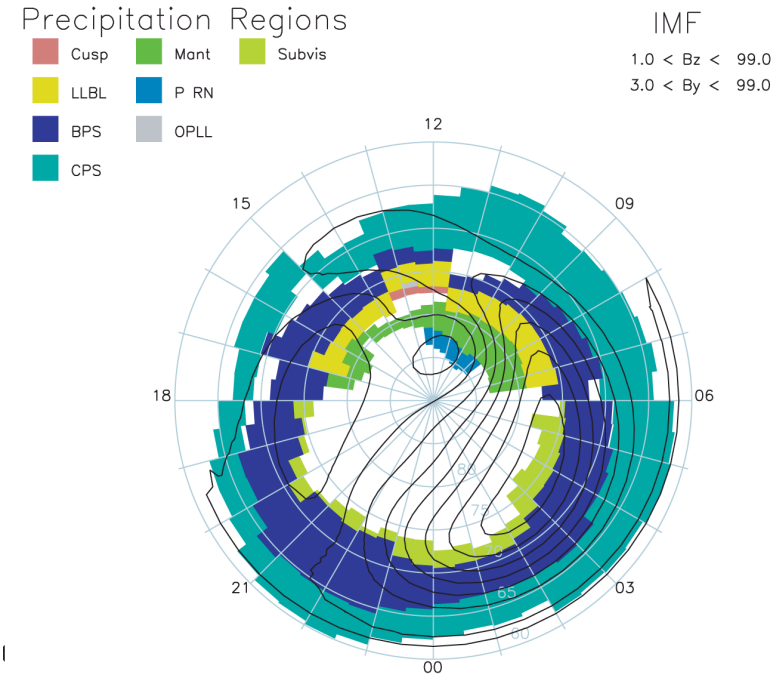

Figure 1: Adapted from Newell et al. [2004]. Eleven years of data from the Defense Meteorological Satellite Program (DMSP) satellites were selected for IMF Bz and By positive conditions. The data have been processed to identify magnetospheric precipitation regions. These method described in the paper identifies the cusp, low latitude boundary layer (LLBL), boundary plasma sheet (BPS), central plasma sheet (CPS), mantel (Mant), polar rain (P RN), open low latitude boundary layer (OPLL), and sub-visual aurora (Subvis) regions. The black contours superimposed on the image are inertial convection streamlines derived from SuperDARN radar data as explained in the paper.

At altitudes near and above the apogee of the Polar satellite (~9R_E geocentric) magnetospheric investigators (e.g., Zhou, et al., 2000, Lavraud et al., 2002, 2004, 2005a, 2005b, Cargill et al., 2005, and Niehof et al., 2008) use magnetic field and plasma observations to identify the "cusp". The high altitude region they call the cusp is identified by a depression of the magnetic field strength below the neighboring background level. Often additional observational details such as a diamagnetic cavity, sudden increase in low-energy ion and electron density, electron thermal energy less than 100 eV, or the presence of significant He^{++} are used to confirm high altitude cusp identification. As shown in Figure 1 of Zhou et al., (2000) magnetic depressions associated with diamagnetic cavities actually determine the region they identify as the high altitude cusp at Polar apogee. See Lavraud et al., (2005a) for maps of the high-altitude cusp properties.

Both definitions of the cusp are in general use. The ionospheric community primarily uses the low altitude, reconnection based cusp definition while the

magnetospheric community primarily uses the high altitude cusp definition. For clarity in this paper we follow the example of Niehof et al., (2008) and use the term Chapman Ferraro Cusp (CFcusp) to identify the region identified as the high altitude cusp.

Fritz and his colleagues (e.g., Chen and Fritz, 1998, Chen and Fritz, 2002, Fritz et al. 2003, and others) suggest that a new process is required to explain recent observations of ~100 keV ionospheric ions in the high altitude CFcusp region. The region Fritz and his colleagues identify using terms such as "cusp", "regions where cusp energetic particle (CEP) events occur", "large-scale, dayside, cusp diamagnetic cavity", and "Chapman-Ferraro cusp" are identical to what we and Niehof et al., (2008) call the CFcusp. Fritz et al. (1993) state: "…by their geometry CFcusp magnetic field lines are connected to all of the magnetopause boundary layers." Lavraud et al., (2005b) also note that the high altitude CFcusp contains mantle and boundary layer plasmas. This is not true of (low altitude) cusp field lines, which originate from the dayside reconnection regions and are identified by only newly injected, cool solar wind plasma.

Ambiguities introduced by the inconsistent definitions of the low altitude cusp and the high altitude CFcusp lead to the inconsistent result that at low altitudes the cusp does not contain boundary layer plasmas, but at high altitudes it does. Fritz and his colleagues assert that a new processes is required to explain the existence of ~100 keV ionospheric ions in the high altitude cusp CFcusp. This assertion ignores research that shows that ~100 keV ionospheric ions can be and are often found in dayside magnetospheric boundary layers. No new processes are required to explain their existence there.

Below we briefly review ionospheric energization and transport processes in the magnetosphere. We then examine the ionospheric plasma found in the high altitude CFcusp in two intervals reported by Fritz and his colleagues and show that these intervals are mixtures of newly reconnected solar wind and boundary layer plasmas.

Ionospheric ion energization and transport

There have been many excellent reviews on extraction and transport of ionospheric plasma and its role in magnetospheric processes (e.g. Yau and André, 1997; André and Yau, 1997; Hultqvist et al., 1999; and Paschmann et al., 2002). Notable advances since these reviews have focused on O^+ energization and transport (Seki et al., 2001, Bouhram et al., 2004, Chaston et al., 2004, Andersson et al., 2005, Strangeway et al., 2005, Nilsson et al., 2006, and Peterson et al., 2008). Acceleration and energization of ionospheric He^+ has been less widely investigated (e.g. Collin et al., 1988 and Lund et al., 1999) but it is generally agreed that the processes responsible for energization and transport are the same for He^+ and O^+.

Thermal (<1eV) ions in the ionosphere are energized by a series of processes that include, pre-heating by photoelectrons, auroral electrons, and Joule heating and additional heating and energization by plasma instabilities, wave particle interactions, parallel electric fields, and centrifugal acceleration in various combinations. Peterson et al., (1992) and Miyake et al., (1993) have shown that wave particle interactions transfer significant (>

100eV) energy to O^+ at all local times and over extended altitude ranges. Sharp et al., (1981), Lindstedt et al., (2010) and others have shown that O^+ energization extends to the outer regions of the magnetosphere, but there are no reports of wave particle energization above ~ 10 keV in spite of the systematic attempts that have been made to find 100 keV O^+ energized by wave particle interaction. For example, Pickett et al., (1999) assembled a comprehensive set of wave and particle observations on the dayside over a wide altitude range to determine if wave particle interactions in the low altitude cusp and CFcusp regions could produce the MeV He^+ ions reported by Chen and Fritz, (1998). The investigators were unable to determine what role, if any, low frequency electromagnetic waves played in producing MeV He^+ ions in the CFcusp. Several authors (e.g. Chen and Fritz, 1998, Chen, 2008, and Vogiatzis, 2008) have shown correlations between the magnetic turbulence spectra in the ULF range and the intensity of the 100 keV He^+ and/or O^+ flux in the CFcusp and/or explored the resonance heating in and near the CFcusp using the method proposed by Chang et al. (1986). None of these papers, however, presents a quantitative argument that directly relates observable plasma wave properties to observed ion energies in the 100 keV range

O^+, H^+, and He^+ ions with >100 keV energies are commonly found in the inner magnetosphere outside of geosynchronous orbit particularly after geomagnetic storms (e.g. Korth et al., 2000). The processes producing these energetic ions involve transport from the plasma sheet and an adiabatic heating process that conserves the first, but not the second, adiabatic invariant (e.g. Hultqvist et al., 1999). In the plasma sheet O^+ and He^+ ions have characteristic energies on the order of 1 keV in a magnetic field of intensity ~10 nT (e.g. Peterson et al., 1981). Earthward convection driven by the cross tail electric field and other processes bring plasma sheet ions into the inner magnetosphere where the magnetic field intensity is on the order of 1, 000 nT. Conservation of the first adiabatic invariant increases the O^+ and He^+ energies to the order of 100 keV. Simulations (e.g. Delcourt and Sauvaud, 1999) confirm that these processes are robust. Asikainen and Mursula (2005, 2006) have examined energetic (30 keV to 4 MeV) protons observed in the high-latitude dayside magnetosphere. Their results suggest that the high-latitude dayside plasma sheet is the main source of energetic particles in the high altitude cusp.

Boundary layer plasmas are mixtures of cool solar wind plasma and hot magnetospheric plasma as discussed in Hultqvist et al., (1999) and references therein. Boundary layer plasmas are found at all latitudes and extend over the entire dayside magnetosphere and down the magnetospheric tail. O^+ and He^+ enters the boundary layer at all local times as part of the hot magnetospheric plasma (e.g. Peterson et al., 1982, Fuselier et al., 1989, Delcourt and Sauvaud, 1999). As shown in Figure 1, Newell et al., (2004) find that boundary layer plasmas are commonly found directly adjacent to cusp plasma at DMSP altitudes. Delcourt and Sauvaud (1999) explicitly show how ~100 keV ionospheric ions are injected into the high altitude CFcusp.

Peterson (1985) reviewed early observations of energetic ions in the low altitude cusp and presented data from DE-1 showing how the solar wind plasma was injected and dispersed under the influence of large-scale magnetospheric convection. Peterson also noted

the close relationship of the upward acceleration of oxygen ions and cusp boundaries. Peterson et al., (1989), André et al., (1990), and Knudsen et al. (1988) demonstrated that a significant portion of the O^+ energization in the cusp could be explained by resonant heating by the broad-band waves commonly found in the cusp using the relationship derived by Chang et al., (1986). Strangeway (2005) examined the relationship between dayside energy inputs and O^+ escape rates on the FAST satellite. He found typical O^+ energies at ~3,000 km less than 100 eV. Peterson et al., (2008) derived the characteristic energy of O^+ in the noon sector at ~2 R_E from instruments on the Polar satellite and found them to be on the order of a few hundred eV. The tails of O^+ distributions in the cusp (not CFcusp) extend to high energies, but there are no reported observations of ~100 keV O^+ ions in or adjacent to regions of newly injected solar wind plasma. The limited observations of He^+ reported by Collin et al., (1988) and Lund et al., (1999) are consistent with O^+ observations summarized here.

Above we have established that O^+ and He^+ transport from the plasma sheet can account for > 100 keV O^+ and He^+ ions in the dayside boundary layers and that observed plasma wave intensities have not been quantitatively demonstrated capable of producing O^+ or He^+ ions with energies of this magnitude. We now examine two intervals where energetic (~ 100 keV) ionospheric ions and were obtained in the CFcusp by Fritz and his colleagues.

Energetic O^+ in the CFcusp on August 3-4, 1997

Figure 2 (reproduced from Chen and Fritz, 2002) shows the flux of 70-200 keV oxygen with charge states 1 and 2 observed on the Polar satellite as it traversed dayside magnetosphere on August 4, 1997 at ~8 R_E geocentric distance. The bottom panel shows the magnetic field intensity. A large-scale diamagnetic cavity is identified from ~ 01:00 to ~02:15 by the depression of and fluctuations in the magnetic field intensity. Chen and Fritz identify the interval from 01:15 to 02:15 UT as a characteristic Cusp Energetic Particle (CEP) event. This interval or an interval slightly expanded in time meets the criteria defining the CFcusp as discussed above. The top panel shows in omni-directional 70-200 keV primarily, as discussed more fully below, O^+ flux observed by the Polar/CAMMICE instrument (see Chen et al., 1998 for some instrumental details). Of particular interest for the present discussion, the CAMMICE temporal resolution is 96s.

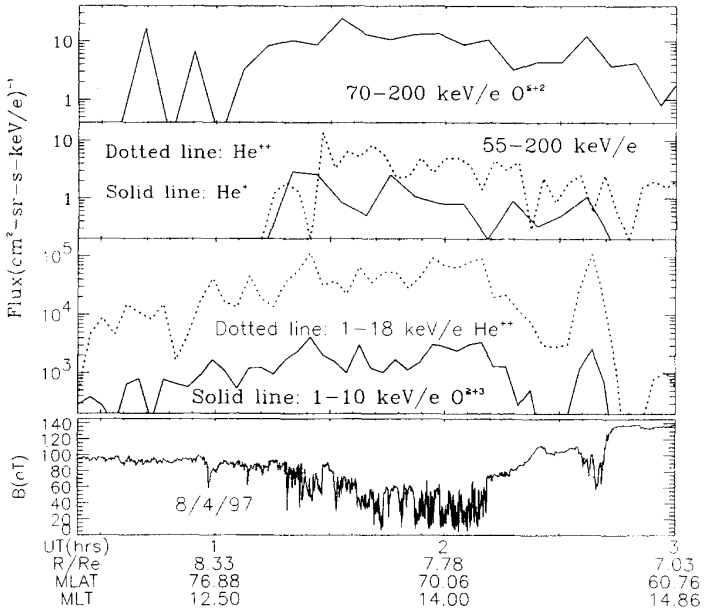

Figure 2: From Chen and Fritz [2002]. Data from the CAMMICE instrument on the Polar spacecraft acquired on August 4, 1997 are displayed. The panels from top to bottom show the variation of the 96 s spin-averaged fluxes of the 70-200 keV/e $O^{\leq+2}$, the 55-200 keV/e He^{++} (dotted line) and He^+ (solid line), the l-10 keV/e $O^{\geq+}3$ (solid line) and 1-18 keV/e He^{++} (dotted line), and the local geomagnetic field versus time, respectively, during the event period. The universal time of data acquisition (UT), geocentric distance of POLAR (in ***R_E),*** the magnetic latitude (MLAT), and the magnetic local time (MLT) are shown at the bottom of the figure. As explained in the text the $O^{\leq+2}$ data are primarily O^+.

Figure 3 shows the average Omni-directional number flux as a function of energy per charge for a number of species for the interval from 1:15 to 2:15 on August 4, 1997. The solid circles in Figure 3 show the observed fluxes of the mass resolved oxygen with charge states 1 and 2; the open squares show H^+, and the open diamonds show He^{++} detected by the CAMMICE instrument during this interval. Solar and geomagnetic activity is modest during

this interval. The $F_{10.7}$ index was below 80. There was moderate geomagnetic activity with the K_P index peaking at 5 at 14:00 on August 3 and decreasing after that. As discussed more fully below, prior geomagnetic activity indicates that a modest amount of O^+ was injected into the magnetosphere and that the charge state of oxygen detected by CAMMICE is primarily O^+.

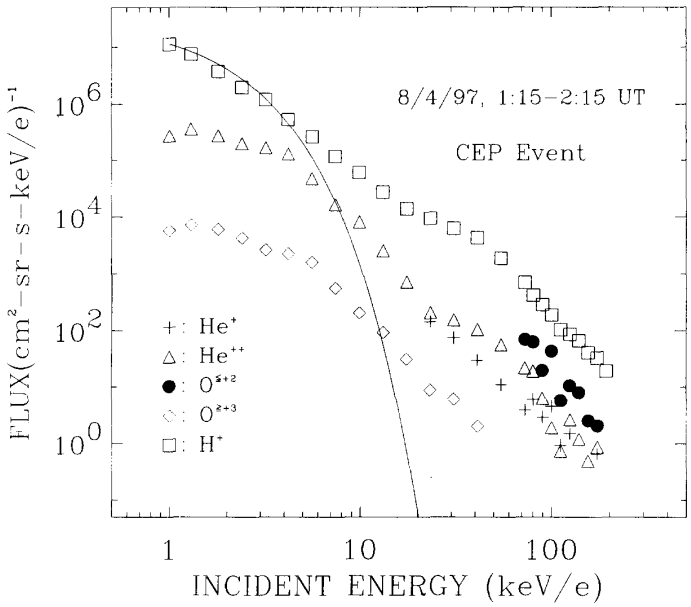

Figure 3: From Chen and Fritz [2002]. The average proton, helium and oxygen energy spectra obtained from 1:15 to 2:15 UT on August 4, 1997. Data from the channel that is sensitive to $O^{\leq+2}$, which is primarily O^+, as explained in the text, are indicated by the solid circles. The solid line is a 1 keV/e Maxwellian energy distribution for solar wind H^+.

The relationship between boundary layer (including mantle) and newly injected solar wind plasmas is shown in Figure 4. Data from the Toroidal Imaging Mass Angle Spectrograph (TIMAS) on the Polar spacecraft (Shelley et al., 1995) from 2100 UT on August 3 to 0500 UT on August 4, 1997 are shown. The data includes the time intervals shown in Figures 2 and 3. The three-color panels in Figure 4 show the omni-directional number flux over the energy range from 15 eV/e to 33 keV/e for H^+, O^+ and He^{++} encoded using the color bar on the right. The bottom panel shows the H^+ flux in units of ions/cm^2-s-sr-keV from the 100 eV channel as a function of time. There was a data drop out shortly after 02:00 when the instrument switched to a mode that did not include sampling of the He^{++} population. The white patches of H^+ flux shown at ~01:30 and ~03:00 indicate regions where the flux H^+ flux is greater than 10^8 ions/cm^2-s-sr-keV/e. This is also indicated in the bottom panel. As noted by Newell and his colleagues regions of newly injected cool solar wind H^+ fluxes are clearly distinguished from the adjacent boundary layer plasmas because they have their maximum fluxes at lower energies. Following Newell and his colleagues we define these two regions of 100 eV H^+ flux intensity above 10^8 as times when the Polar spacecraft flew through newly injected solar wind plasma on this day.

The mixing of solar wind and magnetospheric plasma characteristic of the boundary layer is clearly evident in Figure 4. Boundary layer and/or mantle plasmas extend from

~22:30 on August 3 where significant fluxes of ~200 eV solar wind He^{++} and ~ 100 eV solar wind H^+ fluxes are first observed to ~0330 on August 4 where there is a decrease in the intense ~100 eV solar wind H^+ flux. We note that the character of the omni-directional O^+ equatorward of the boundary layer seen in Figure 4 is significantly different on August 3, when Polar is in the high-latitude, high-altitude, morning side region than it is on August 4, when Polar is at lower altitudes and latitudes in the afternoon region.

Figure 4: Data from the TIMAS instrument on the Polar spacecraft obtained from 21:00 on August 3, 1997 to 05:00 on August 4, 1997. The 3 color panels show the observed omni-directional number flux in units of $(cm^2\text{-s-sr-keV/e})^{-1}$ encoded by the color bar on the right for H^+, O^+ and He^{++} respectively. The energy range of the data is from 15 eV/e to 33 keV/e. The bottom panel displays the observed omni-directional H^+ flux from the 100 eV channel. Universal time (UT), geocentric distance (R), eccentric dipole magnetic local time (EDMLT), and geomagnetic latitude (MAGLAT) are shown at the bottom. Vertical green lines are at 01:15 and 02:15 bounding the region identified by Chen and Fritz [2002] as the CF cusp.

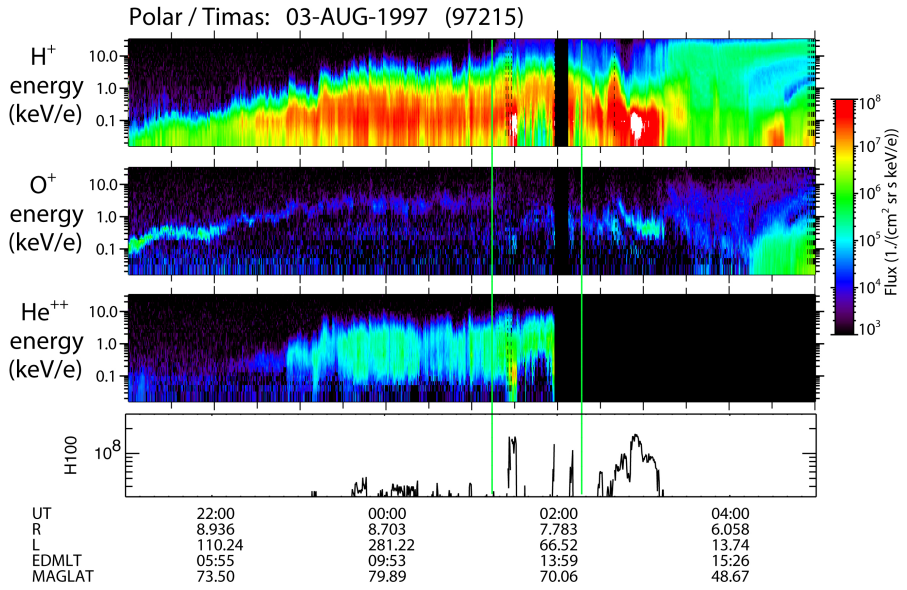

Figure 4: Data from the TIMAS instrument on the Polar spacecraft obtained from 21:00 on August 3, 1997 to 05:00 on August 4, 1997. The 3 color panels show the observed omni-directional number flux in units of $(cm^2\text{-s-sr-keV/e})^{-1}$ encoded by the color bar on the right for H^+, O^+ and He^{++} respectively. The energy range of the data is from 15 eV/e to 33 keV/e. The bottom panel displays the observed omni-directional H^+ flux from the 100 eV channel. Universal time (UT), geocentric distance (R), eccentric dipole magnetic local time (EDMLT), and geomagnetic latitude (MAGLAT) are shown at the bottom. Vertical green lines are at 01:15 and 02:15 bounding the region identified by Chen and Fritz [2002] as the CF cusp.

Figure 5 shows solar wind information from the Wind spacecraft for the interval shown in Figure 4. The Wind data have been time lagged to account for propagation between Wind and the magnetosphere. The top panel shows density (dark) and pressure (light) indicating a sharp density and pressure increase at ~2:30. The middle panel shows that the solar wind velocity was constant at about 400 km/s for this interval. The interplanetary magnetic field in

the bottom panel shows that Bz (red) was positive through out the interval and Bx (black) was relatively small and negative. By (green) was strongly positive before ~02:30 where it turned abruptly negative and slowly rotated back positive.

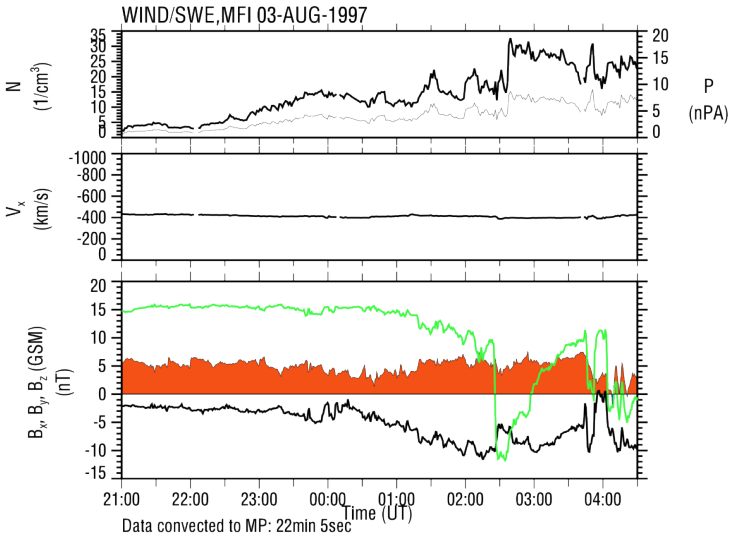

Figure 5: Solar wind density, pressure, and magnetic field data from the Wind spacecraft obtained on August 3 and 4, 1997. The data have been time shifted by 22 minutes and 5 seconds to account for the convection time from Wind to the magnetopause. The top panel shows density (solid line) and pressure (light line). The second panel shows the solar wind velocity. The bottom panel shows the solar wind magnetic field components in GSM coordinates: Bx (black), By (green), and Bz (red). Data from the ACE spacecraft are not available until later in 1997.

The cusp is dynamic. As noted above, the intense fluxes at ~1:30 and ~3:00 are times that the Polar satellite was on newly reconnected field lines. At other times Polar was on field lines containing boundary layer and/or mantle plasmas evidenced by the heated solar wind H^+ and He^{++} and O^+ populations. The location of the reconnection site depends strongly on the IMF direction as described by Trattner et al., (2007) and references therein. The location also depends on the solar wind density and/or pressure. The location of newly reconnected plasma at ~1:30 and ~3:00 in the TIMAS data reflect the changing solar wind conditions and are consistent with previous observations. The O^+ populations seen before ~01:00 and from ~02:30 to ~3:30 are primarily field aligned and flowing upward from the ionosphere below. Krauklis et al., (2001a, 2001b) have discussed these O^+ distributions and the physical processes responsible for producing them. Between 01:00 and 02:30 and after 3:30 the O^+ angular distributions are more complex. Our primary interest in the data shown in Figures 4 and 5 is the interval from 01:15 to 02:15 identified by Chen and Fritz as the high altitude CFcusp.

The 24 s time resolution TIMAS data shown in Figure 4 show that the Polar satellite was on newly reconnected field lines from 01:23:50 to 01:31. The data also show that Polar was

on boundary layer and mantle field lines from 22:30 on August 3 to 01:23:50 on August 4, and again from 01:31 to ~3:30 on August 4. Figure 6 presents average omni-directional H^+(red), He^{++}(blue), and O^+(black) energy spectra for four time intervals including the CFcusp (from 01:15 to 02:15 indicated by the dashed lines), when TIMAS was observing newly reconnected solar wind plasma (identified by solid lines), and when TIMAS was observing boundary layer and/or mantle plasma, indicated by dotted lines, and a post-noon outer magnetospheric interval (from 03:30 to 03:50) indicated by the dash dot lines). Other investigators have also noted gradients in ionospheric ions with energies in the 10's of keV in and near the low (e.g. Kremser et al., 1995) and high-altitude CFcusp (e.g. Lavraud et al., 2005b) suggestive of a boundary layer source.

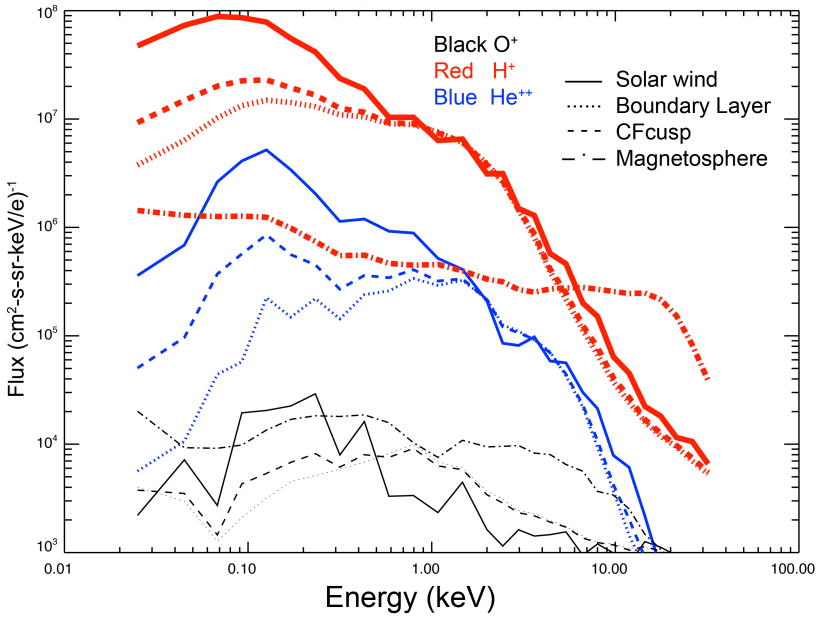

Figure 6: Average O^+ (black), H^+ (red), and He^{++} (blue) energy spectra observed by the TIMAS instrument in various magnetospheric regions on August 4, 1997. The average energy flux in the region of newly reconnected solar wind plasma is indicated by solid lines; in the boundary layer region it is indicted by dotted lines. The average energy flux in the high altitude CFcusp region is indicated by the dashed line. Newly injected solar wind (cusp) plasma was observed from 01:23:50 to 01:31. CFcusp plasma was observed from 01:15 to 02:15. Boundary layer plasma shown was obtained from 01:15 to 02:15 and does not include the interval of newly injected solar wind (cusp) plasma. The red and black dot dashed line shows the average H^+ and O^+ energy spectra obtained in the magnetosphere from 03:30 to 03:50.

Differences in CFcusp, cusp (i.e. newly reconnected solar wind plasma), and boundary layer/mantle plasmas are most clearly distinguished in the He^{++} fluxes in Figure 6. Similar, but less pronounced, differences between CFcusp, boundary layer, and cusp H^+ plasmas are seen in Figure 6. H^+ fluxes at ~30 keV/e detected by TIMAS have a magnitude of ~10^4 ions/cm^2-s-sr-keV in the newly reconnected solar wind, CFcusp, and boundary layer intervals consistent with the H^+ fluxes reported in Figure 3 from the CAMMICE instrument. As discussed below, the CFcusp O^+ fluxes at 10 keV detected by TIMAS are also consistent with the $O^{\leq 2+}$ fluxes at 70 keV reported in Figure 3. As expected the energetic (>10 keV) H^+

fluxes in the inner magnetosphere are more intense and show a different energy distribution than the mixture of hot magnetospheric and cold solar wind plasmas found in the boundary layer / mantle.

The CAMMICE instrument cannot distinguish between oxygen ions with charge states 1 and 2. O^{++} is produced primarily by photoionization of magnetospheric O^{+} (Breig, et al., 1977); it does not come directly from the ionosphere. Prior geomagnetic activity, with the K_P index peaking at 5 at 14:00 on August 3 injected O^{+} into the magnetosphere, but the amounts were relatively modest because of the low level of solar activity indicated by an $F_{10.7}$ index below 80 (e.g. Yau et al., 1988). Since the time-constant for photoionization of O^{+} is relatively slow (Breig et al., 1977) and the magnetospheric O^{+} population is expected to be low (Young et al., 1982), the O^{++} population is expected to be significantly less than that of O^{+}.

We note that the CAMMICE and TIMAS flux intensities agree well. The 70 keV/e O^{+} fluxes observed by CAMMICE in the CFcusp shown in Figure 3 have an intensity of ~50 ions/cm^2-s-sr-keV compared to ~1,000 ions/cm^2-s-sr-keV observed by TIMAS at 10 keV/e shown in Figure 6. This rate of O^{+} flux decrease with energy is roughly equivalent to the decrease observed for H^{+} by CAMMICE over a comparable energy range as shown in Figure 2. Similar to the TIMAS H^{+} energy spectrum in the magnetosphere (03:30 to 03:50), the TIMAS magnetospheric O^{+} energy spectrum is significantly hotter than those observed in the CFcusp or boundary layer. Temporal aliasing from sampling O^{+} ions from interleaved energy steps on alternate 6 s satellite spins (Shelley et al., 1995) is apparent in the O^{+} fluxes in Figure 6. This temporal aliasing is indicative of a sharper gradient in O^{+} distribution than in the contemporaneously sampled H^{+} and He^{++} populations.

Energetic He^{+} in the CFcusp on August 27, 1996

The data from August 4, 1997 were obtained under relatively steady solar wind conditions where regions of newly injected solar wind plasma do not move as the location of reconnection changes with IMF direction (e.g. Trattner et al., 2007). To examine the relationship between newly reconnected solar wind and boundary layer plasmas during conditions when the IMF is rapidly changing direction we examine an interval on August 27, 1996, which has previously been analyzed by Niehof et al., (2008). Niehof et al. used data from multiple instruments on the Polar satellite, including the presence of ionospheric He^{+} with energies ~100 keV to identify the high altitude CFcusp from 08:35 to 09:05.

An extended interval of data from the Polar satellite obtained on August 27, 1996 is shown in Figure 7. The top four panels are the same as those shown in Figure 4: omni-directional energy-time spectrograms for H^{+}, O^{+} and He^{+} and a panel showing the H^{+} flux intensity at 100 eV. The bottom panel shows the magnetic field intensity at ~1 minute resolution. A region of reduced magnetic intensity from ~0830 to ~0905 indicates where the CDC and energetic He^{+} were identified by Niehof et al., (2008). We note but do not discuss a second high altitude CFcusp region between ~0930 and ~1000. Here we focus on the interval from 08:00 to 09:30 where the IMF was relatively stable as shown in Figure 8

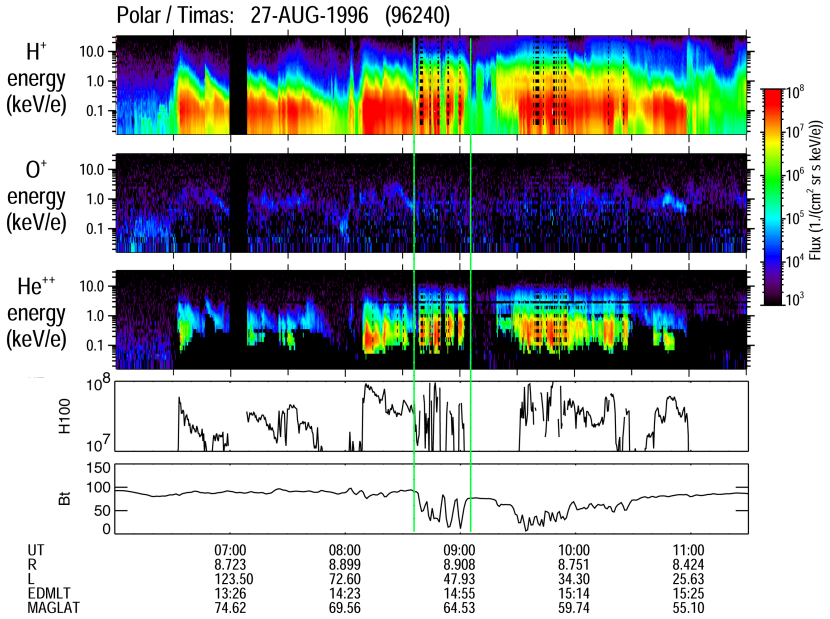

Figure 7: Data from the TIMAS instrument on the Polar spacecraft obtained from 06:00 to 11:30 on August 27, 1996. The 3 color panels show the observed omni-directional number flux for H^+, O^+ and He^{++} respectively in the same format as shown in Figure 4. The fourth panel displays the observed omni-directional H^+ flux from the 100 eV channel. The bottom panel displays the magnetic field intensity in units of nT from the ~ 1 min resolution Polar magnetometer key parameter database. Vertical green lines are at 08:35 and 09:35 bounding the region identified by Niehof et al., [2008] as the CF cusp.

Figure 8 presents solar wind magnetic and plasma data from 08:00 to 09:30 on August 27, 1996 in the same format as Figure 5. The data have been time lagged to account for propagation between Wind satellite and the magnetosphere. The top panel shows density (dark) and pressure (light). The middle panel shows that the solar wind velocity. Solar wind plasma conditions were constant for this interval. The interplanetary magnetic field in the bottom panel shows that Bz (red and blue) was positive after ~0830 and Bx (black) was negative. By (green) was mostly positive during this interval.

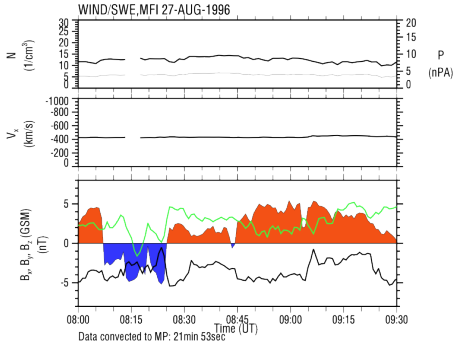

Figure 8: Solar wind density, pressure, and magnetic field data from the WIND spacecraft obtained on August 27, 1996 in the same format as that shown in Figure 5. The data have been time shifted by 21 minutes and 53 seconds to account for the convection time from WIND to the magnetopause.

As noted in the discussion of Figures 4 and 6, newly injected solar wind plasma can be identified in the TIMAS data by the relative intensity of the ~100 eV H^+ flux. We identify the region of newly reconnected solar wind plasma in Figure 7 as the 24 s accumulation intervals in the TIMAS data where the omni-directional H^+ flux intensity is >6 x 10^7 ions/cm^2-s-sr-keV. We use this threshold because the data on August 27, 1996 were obtained at a slightly higher altitude and later local time and under difference geomagnetic conditions than those shown in Figure 6 obtained on August 3-4, 1997.. During the interval of interest from 0800 to 0930 , the 100 eV H^+ flux was above 6 x 10^7 ions/cm^2-s-sr-keV from 0810 to 0821, and intermittently during six of the 24 s accumulation intervals between 0840 and 0850. The other 24 s intervals between 0800 and 0930 are identified as boundary layer and/or mantle.

Figure 9 presents average omni-directional H^+(red), He^{++}(blue), and O^+(black) energy spectra for four time intervals including the CFcusp (from 08:35 to 09:05 indicated by the dashed lines), the region of newly reconnected solar wind plasma (identified by solid lines), and the region with boundary layer and/or mantle plasma, and a post-noon outer magnetospheric interval (from 11:10 to 11:30 indicated by the dash dot lines).

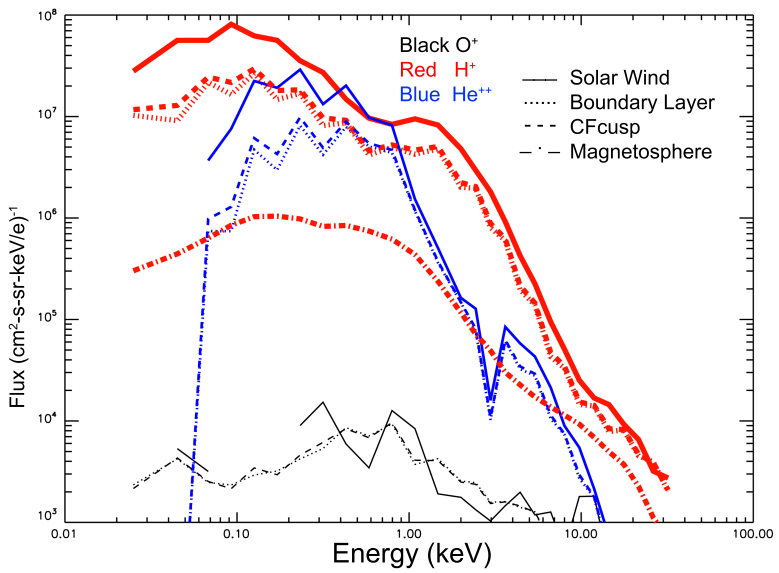

Figure 9. Average H^+, O^+ and He^{++} energy spectra from TIMAS in the same format as Figure 6. The high altitude CFcusp interval identified by Neihof et al., (2008) from 08:35 to 09:05 is indicated by the dashed lines. Newly injected solar wind (cusp) plasma was observed from 0810 to 0821 and intermittently during six of the 24 s accumulation intervals between 0840 and 0850. CFcusp plasma was observed from 08;35 to 09:05. Boundary layer plasma shown was obtained from 08:35 to 09:05 and does not include the interval of newly injected solar wind (cusp) plasma. The H^+ energy spectra obtained from 11:10 to 11:30 in the magnetosphere is indicated by the dot dashed line.

Differences in CFcusp, newly reconnected solar wind, and boundary layer/mantle plasmas are clearly identified in the both the H^+ and He^{++} fluxes in Figure 9. He^{++} and H^+ fluxes in the CFcusp are a mixture of boundary layer/mantle and newly reconnected solar wind plasmas. H^+ fluxes at ~30 keV/e detected by TIMAS have a magnitude of $\sim 10^4$ ions/cm^2-s-sr-keV in the CFcusp and boundary layer consistent with the total ion flux reported by Niehof et al., (2008) for this interval from the CAMMICE instrument. The fluxes of O^+ fluxes are too low for further analysis. The He^+ fluxes (not shown) are at or below the flux threshold of the TIMAS instrument during these intervals.

Summary

We noted how ambiguities introduced by the inconsistent definitions of the low and high altitude cusp lead to the inconsistency that at low altitudes the region commonly known as the cusp does not contain boundary layer plasmas, but at high altitudes it does. We have reviewed the methods used to identify the low and high altitude cusp, boundary layers and mantle in the dayside magnetosphere. We have followed the example of Niehof et al., (2008) and use the term Chapman Ferraro cusp (CFcusp) to identify the high altitude cusp. We presented plasma data from two CFcusp intervals: One interval where the solar wind conditions were steady and one where they were more dynamic. We reviewed the well-known processes that bring energetic (~100 keV) ionospheric ions onto high altitude dayside magnetospheric and boundary layer field lines. We also noted that topologically the CFcusp includes boundary layer and/or mantle plasmas as well as newly reconnected solar wind plasma

We presented data from the CAMMICE and TIMAS instruments on August 3-4, 1997 and August 27, 1996 obtained as the Polar spacecraft flew through the high altitude CFcusp. Well-known and established criteria based on ion flux, peak energy, and composition were used to identify the times the Polar spacecraft was sampling newly reconnected solar wind, boundary layer, and magnetospheric plasmas. We used the presence of warm He^{++} and the lack of newly reconnected solar wind plasma to identify boundary layer plasmas. We confirmed previous observations (e.g. Lavraud et al., 2005b) and simulations (e.g. Delcourt and Savaud, 1999) that the high altitude CFcusp includes both newly injected solar wind and boundary layer plasmas.

We noted that the CAMMICE $O^{<2+}$ energy spectrum in Figure 3 was primarily O^+ and that the TIMAS O^+ and H^+ energy spectra presented in Figure 6 are consistent with CAMMICE spectra shown in Figure 3. No CAMMICE energy spectra for August 27, 1996 were presented by Niehof et al., (2008). However we noted that all the CAMMICE ion (H^+) fluxes given in a color-encoded energy-time spectrogram by Niehof et al. are consistent with the TIMAS H^+ spectra shown in Figure 9.

Figures 6 and 9 show H^+, O^+, and He^{++} fluxes from the two high-altitude Polar satellite intervals investigated. Data from the CFcusp, newly reconnected solar wind and boundary layer plasma regions are presented with energy spectra obtained in the magnetosphere. The H^+ and He^{++} spectra from regions of newly reconnected solar wind plasma in Figures 6 and 9

have their maximum fluxes at lower energies than the boundary layer and CFcusp plasmas. This is the property exploited by Newell and his colleagues to robustly identify the low altitude cusp. The H^+ and He^{++} energy spectra in Figures 6 and 9 from boundary layer intervals are consistent with a mixture of heated solar wind and magnetospheric plasmas. The H^+ and He^{++} energy spectra obtained in the CFcusp and shown in Figures 6 and 9 are clearly a mixture of newly reconnected solar wind and boundary layer plasmas.

Fritz and his colleagues (e.g. Chen and Fritz, 1998, Chen and Fritz, 2002, Fritz et al. 2003, and Niehof et al., 2008) assert that a new process or processes are required to explain energetic (>100 keV/e) He^+, O^+, and solar wind ions observed in the CFcusp. As noted above modest energization of O^+ and He^+ in the cusp can be explained by resonant heating by the broadband waves commonly found there using the relationship derived by Chang et al., (1986). Chen and Fritz, (1998), Chen, (2008), and Vogiatzis, (2008) have shown correlations between the magnetic turbulence spectra in the ULF range and the intensity of the 100 keV He^+ and/or O^+ flux in the CFcusp and/or explored the resonance heating in and near the CFcusp using the method proposed by Chang et al. (1986). None of these papers, however, presents a quantitative argument that directly relates observable plasma wave properties to observed ion energies in the 100 keV range.

We noted that energetic (>100 keV) ionospheric ions are often found in the dayside magnetosphere and adjacent boundary layers. We reviewed the well-known processes responsible for energizing and transporting ionospheric O^+ and He^+ to the plasma sheet and then to the dayside magnetosphere where they can have energies > 100 keV. We concluded that the ~100 keV O^+ reported by Chen and Fritz (2002) and the ~100 keV He^+ reported by Niehof et al., (2008) in the high altitude CFcusp included magnetospheric boundary layer plasmas and that no new process is required to explain the observations.

Niehof et al., (2008) suggested specific local plasma conditions that were necessary in the cusp diamagnetic cavity to energize both ionospheric and solar wind plasmas. Chang et al., (1998, 2000), Trattner et al., (1999, 2001), Fuselier et al., 2009; Trattner et al., (2010), and others have demonstrated that the solar wind ion energy spectra observed downstream from a quasi-parallel shock are similar to those reported by Fritz and his colleagues in the high altitude CFcusp. In particular Trattner et al. (2010) have analyzed several of the high altitude crossings by the Polar satellite during variable IMF conditions some of them previously analyzed by Niehof et al., (2008) and documented local plasma conditions. The Trattner et al. (2010) analysis demonstrated that the occurrence of energetic ions in the CFcusp is not uniquely determined by local plasma conditions. They found, as had previous authors, that the flux of energetic ions depends on the location of the quasi-parallel bow shock and the magnetic topology in the magnetosheath and that no new process is required to explain the observations.

It is indeed unfortunate that there are inconsistent definitions of the low altitude cusp and the high altitude CFcusp. Because they did not adequately account for boundary layer fluxes, these inconsistencies lead Fritz and his colleagues to postulate the need for additional energization mechanisms acting on both solar wind and ionospheric plasma in the day side

magnetosphere. Based on the analysis presented here we conclude that there is no need to postulate an additional process driven by waves in a diamagnetic cavity to energize ionospheric ions to over 100 keV in the CFcusp.

Acknowledgements:

We acknowledge the use of ISTP KP database. Solar wind observations were provided by K. Ogilvie at NASA/GSFC (Wind/SWE). Magnetic field observations were provided by R. Lepping at NASA/GSFC (Wind/MFI). The work at Lockheed Martin was supported by NASA contracts NNG05GE93G, NNX08AF35G, NNG05GE15G and a grant by the National Science Foundation under grant No. 0503201. WKP thanks Laila Andersson and Benoit Lavraud for helpful comments. We thank Ed Shelley who conceived, designed, and built the high quality TIMAS instrument. We also thank one of the reviewers for his careful analysis of the original version of this manuscript.

References:

Andersson, L, W.K. Peterson, and K.M. McBryde (2005), Estimates of the suprathermal O + outflow characteristic energy and relative location in the auroral oval, Geophys. Res. Lett., 32, L09104, doi:10.1029/2004GL021434.

André, M., G.B. Crew, W.K. Peterson, A.M. Persoon, C.J. Pollock, and M.J. Engebretson (1990), Heating by Broadband Low-Frequency Waves in the Cusp/Cleft, J. Geophys. Res. 95, 20809.

André, M. and A.W. Yau (1997), Theories and observations of ion energization and outflow in the high latitude magnetosphere, Space. Sci. Rev., 80, 26.

Asikainen, T. and K. Mursula (2005), Energetic particle fluxes in the exterior cusp and the high-latitude dayside magnetosphere: statistical results from the Cluster/RAPID instrument, Annales Geophysicae, 23, 2217–2230.

Asikainen, T. and K. Mursula (2006), Reconnection and energetic particles at the edge of the exterior cusp, Ann. Geophys., 24, 1949–1956.

Bouhram, M., B. Klecker, G. Paschmann, H. Rème, A. Blagau, L. Kistler, P. Puhl-Quinn, and J. Sauvaud (2004), Multipoint analysis of the spatiotemporal coherence of dayside O+ outflows with Cluster, Ann. Geophys., 22, 2507–2514.

Breig, E. L., M. R. Torr, D. G. Torr, W. B. Hanson, J. H. Hoffman, J. C. G. Walker, and A. O. Nier (1977), Doubly Charged Atomic Oxygen Ions in the Thermosphere, 1. Photochemistry, *J. Geophys. Res.*, *82*(7), 1008–1012, doi:10.1029/JA082i007p01008.

Cargill, P. J., B. Lavraud, C. J. Owen, B. Grison, M. W. Dunlop, N. Cornilleau-Wehrlin, C. P. Escoubet, G. Paschmann, T. D. Phan, L. Rezeau, Y. Bogdanova, and K. Nykyri (2005), Cluster at the Magnetospheric Cusps, Space Sci. Rev., 118, No. 1-4, 321-366, doi:10.1007/s11214-005-3835-0.

Chang, T., G.B. Crew, N. Hershkowitz, J.R. Jasperse, J.M. Retterer, and J.D. Winningham (1986), Transverse acceleration of oxygen ions by electromagnetic ion cyclotron resonance with broad band left-hand polarized waves, Geophys. Res. Lett., 13, 636.

Chang, S.-W., J.D. Scudder, S.A. Fuselier, J.F. Fennell, K.J. Trattner, J.S. Pickett, H.E. Spence, W.K. Peterson, C.T. Russell, R.P. Lepping, and R. Friedel (1998), Cusp energetic ions: A bow shock source, Geophysical Research Letters 25. 3729.

Chang, S.-W., J.D. Scudder, J.F. Fennell, R. Friedel, R.P. Lepping, C.T. Russell, K.J. Trattner, S.A. Fuselier, W.K. Peterson, and H.E. Spence (2000), Energetic

magnetosheath ions connected to the Earth's bow shock: Possible source of CEP's, *J. Geophys. Res., 105*, 5471-5488.

Chaston, C. C., J. W. Bonnell, C. W. Carlson, J. P. McFadden, R. E. Ergun, R. J. Strangeway, and E. J. Lund (2004), Auroral ion acceleration in dispersive Alfvén waves, J. Geophys. Res., 109, A04205, doi:10.1029/2003JA010053.

Chen, J., and T. A. Fritz (1998), Correlation of cusp MeV helium with turbulent ULF power spectra and its implications, Geophys. Res. Lett., 25(22), 4113-4116.

Chen, J, T.A. Fritz, R.B. Sheldon, H.E. Spence, W.N. Spjeldvik, J.F. Fennel, S. Livi, C.T. Russell, J.S. Pickett, and D.A. Gurnett (1998), Energetic particle events: Implications for a major acceleration region of the magnetosphere, J. Geophys. Res., 103, 69.

Chen, J. and T.A. Fritz, Cusp energetic oxygen ions of ionospheric origin (2002), Adv. Space Res., 30, 29611.

Chen, J. (2008), Evidence for particle acceleration in the magnetospheric cusp, Ann. Geophys., 26, 1993-1997.

Collin, H.L., W.K. Peterson, J.F. Drake, and A.W. Yau (1988), The Helium Components of Energetic Terrestrial Ion Upflows: Their Occurrence, Morphology, and Intensity, J. Geophys. Res. 93, 7558.

Cowley, S.W.H., The cause of convection in the Earth's Magnetosphere: A Review of developments during the IMS, *Rev. Geophys. Res., 20*, 531-565, 1982.

Delcourt, D.C, and J.-A. Sauvaud (1999), Populating of the cusp and boundary layers by energetic (hundreds of keV) equatorial particles, J. Geophys. Res., 104, 22635.

Fritz, T. A., J. Chen, and G. L. Siscoe (2003), Energetic ions, large diamagnetic cavities, and Chapman-Ferraro cusp, *J. Geophys. Res.*, 108(A1), 1028, doi:10.1029/2002JA009476.

Fuselier, S. A., D. M. Klumpar, W. K. Peterson, and E. G. Shelley (1989), Direct injection of ionospheric O^+ into the dayside low latitude boundary layer, *Geophys. Res. Lett.*, 16(10), 1121–1124, doi:10.1029/GL016i010p01121.

Fuselier, S.A., D.M. Klumpar, and E.G. Shelley, Ion reflection and transmissions during reconnection at the Earth's subsolar magnetopause, *Geophys. Res. Lett., 18*, 139-142, 1991.

Fuselier, S.A., S.M. Petrinec and K.J. Trattner (2009), Comment on "Energetic particles sounding of the magnetospheric cusp with ISEE-1" by K.E. Whitaker et al., Ann. Geophysicae, 25, 1175-1182, 2007, *Ann. Geophys., 27*, 441-445.

Gosling, J.T., M.F. Thomsen, S.J. Bame, R.C. Elphic, and C.T. Russell, Cold ion beams in low-latitude boundary layer during accelerated flow events, *Geophys. Res. Lett., 17*, 2245-2248, 1990.

Heikkila, W.J., Definition of the cusp (1985)), J.A. Holtet and A. Egeland (eds.), The Polar Cusp, D. Reidel, p.387-395.

Hultqvist, B, M. Øieroset, G. Paschmann, and R. Treuman Editors (1999), *Magnetospheric plasma sources and losses*, Kluwer Academic Publishers, Dordrecht/Boston/London.

Knudsen, D. J., J. H. Clemmons, and J.-E. Wahlund (1998), Correlation between core ion energization, suprathermal electron bursts, and broadband ELF plasma waves, *J. Geophys. Res.*, *103*(A3), 4171–4186, doi:10.1029/97JA00696.

Korth, A, R.H.W. Friedel, C.G. Mouikis, J.F. Fennell, J.R. Wygant, and H. Korth (2000), Comprehensive particle and field observations of magnetic storms at different local times from the CRRES spacecraft, J. Geophys. Res., 105, 18729.

Krauklis, I., A.J. Coates, and W.K. Peterson (2001a), Magnetic local time dependency of cusp ion velocity dispersions in the mid-altitude cusp, I. Krauklis, Geophys. Res. Lett, 28, 4057.

Krauklis, I, A.D. Johnstone, and W.K. Peterson (2001b), The acceleration of ionospheric O^+ ions on open field Lines in the LLBL and cusp region, J. Geophys. Res, 106, 29611.

Kremser, G., J. Woch, K. Mursula, P. Tanskanen, B. Wilken, and R. Lundin (1995), Origin of Energetic Ions in the Polar Cusp Inferred from Ion Composition Measurements by the Viking satellite, Ann. Geophys. 13, 595.

Lavraud, B., M. W. Dunlop, T. D. Phan, H. Rème, J. M. Bosqued, I. Dandouras, J.-A. Sauvaud, R. Lundin, M. G. G. T. Taylor, P. J. Cargill, C. Mazelle, C. P. Escoubet, C. W. Carlson, J. P. McFadden, G. K. Parks, E. Moebius, L. M. Kistler, M.-B. Bavassano-Cattaneo, A. Korth, B. Klecker and A. Balogh (2002)., Cluster observations of the exterior cusp and its surrounding boundaries under northward IMF, Geophys. Res. Lett., 29, No. 20, 56.

Lavraud, B., A. Fedorov, E. Budnik, A. Grigoriev, P. J. Cargill, M. W. Dunlop, H. Rème, I. Dandouras, and A. Balogh (2004), Cluster survey of the high-altitude cusp properties: A three-year statistical study, Ann. Geophys., 22, No. 8, 3009-3019.

Lavraud, B., A. Fedorov, E. Budnik, M. F. Thomsen, A. Grigoriev, P. J. Cargill, M. W. Dunlop, H. Rème, I. Dandouras, and A. Balogh (2005a), High-altitude cusp flows dependence on IMF orientation: A three-year Cluster statistical study, J. Geophys. Res., 110, A02209, doi:10.1029/2004JA010804.

Lavraud, B, et al. (2005b), Cluster observes the high-altitude cusp region, Surveys in Geophys, 26, 135, doi:10.1007/s10712-005-1875-3.

Lindstedt, T., Y. V. Khotyaintsev, A. Vaivads, M. André, H. Nilsson, and M. Waara (2010), Oxygen energization by localized perpendicular electric fields at the cusp boundary, Geophys. Res. Lett., 37, L09103, doi:10.1029/2010GL043117.

Lotko, W (2007), The magnetosphere-ionosphere system from the perspective of plasma circulation: A tutorial, J. Atmos. Solar Terr. Phys., 69, 191.

Lund, E. J., E. Möbius, D. M. Klumpar, L. M. Kistler, M. A. Popecki, B. Klecker, R. E. Ergun, J. P. McFadden, C. W. Carlson, and R. J. Strangeway (1999), Direct comparison of transverse ion acceleration mechanisms in the auroral region at solar minimum, *J. Geophys. Res.*, 104(A10), 22,801–22,805, doi:10.1029/1999JA900265.

Meng, C.-I, and M. Candidi, Polar cusp features observed by DMSP satellites (1985) , The Polar Cusp, D. Reidel, p.177-192

Miyake, W., T. Mukai, and N. Kaya (1993), On the Evolution of Ion Conics Along the Field Line From EXOS D Observations, *J. Geophys. Res.*, *98*(A7), 11,127–11,134, doi:10.1029/92JA00716.

Newell, P.T. and C.-I. Meng, The cusp and cleft/boundary layer: Low-altitude idenification and statistical local time variation (1988), J. Geophys. Res., 93, 14549.

Newell, P.T., and C.-I. Meng, On quantifying the distinctions between the cusp and the cleft/LLBL (1989), P.E. Sandholdt and A. Egeland (eds.), Electromagnetic Coupling in the Polar Clefts and Caps, Kluwer Academic Publishers, p.87-101.

Newell, P. T., J. M. Ruohoniemi, and C.-I. Meng (2004), Maps of precipitation by source region, binned by IMF, with inertial convection streamlines, J. Geophys. Res., 109, A10206, doi:10.1029/2004JA010499.

Niehof, J. T., T. A. Fritz, R. H. W. Friedel, and J. Chen (2008), Interdependence of magnetic field and plasma pressures in cusp diamagnetic cavities, Geophys. Res. Lett., 35, L11101, doi:10.1029/2008GL033589.

Nilsson, H., et al. (2006), Characteristics of high altitude oxygen ion energization and outflow as observed by Cluster: A statistical study, Ann. Geophys., 24, 1099–1112.

Palmroth, M, P. Janhunen, T.I. Pulkkinen, and W.K. Peterson (2001), Cusp and magnetopause locations in global MHD simulation, J. Geophys. Res., 106, 29435.

Paschmann, G, S. Haaland, and R. Treumann Editors (2002), *Auroral Plasma Physics*, Kluwer Academic Publishers, Dordrecht/Boston/London

Peterson, W.K., R.D. Sharp, E.G. Shelley, R.G. Johnson, and H. Balsiger, (1981) Energetic Ion Composition of the Plasma Sheet, J. Geophys. Res. 86, 761.

Peterson, W. K., E. G. Shelley, G. Haerendel, and G. Paschmann (1982), Energetic Ion Composition in the Subsolar Magnetopause and Boundary Layer, *J. Geophys. Res.*, 87(A4), 2139–2145, doi:10.1029/JA087iA04p02139.

Peterson, W.K, Ion injection and acceleration in the polar cusp (1985), J.A. Holtet and A. Egeland (eds.), *The Polar Cusp,* D. Reidel, p.67-84.

Peterson, W.K., M. André, C.B. Crew, A.M. Persoon, M.J. Engebretson, C.J. Pollock, and M. Temerin (1989), Heating of thermal ions near the equatorward boundary of the mid-altitude polar cleft, P.E. Sandholdt and A. Egeland (eds.), Electromagnetic Coupling in the Polar Clefts and Caps, Kluwer Academic Publishers, p.103-113.

Peterson, W.K., H.L. Collin, M.F. Doherty, and C.M. Bjorklund (1992), O^+ and He^+ restricted and extended (bi-modal) ion conic distributions, Geophys. Res. Lett., 19, 1439.

Peterson, W.K., T. Abe, M. André, M.J. Engebretson, H. Fukunishi, H. Hayakawa, A. Matsuoka, T. Mukai, A.M. Persoon, J.M. Retterer, R.M. Robinson, M. Sugiura, K. Tsuruda, D.D. Wallis, and A.W. Yau (1993), Observations of a transverse magnetic field perturbation at two altitudes on the equatorward edge of the magnetospheric cusp, J. Geophys. Res. 98, 21463.

Peterson, W.K., L. Andersson, B.C. Callahan, H.L. Collin, J.D. Scudder, and A.W. Yau (2008), Solar-minimum quiet-time ion energization and outflow in dynamic boundary related coordinates, J. Geophys. Res. 113, A07222, doi:10.1029/2008JA013059.

Pickett, J.S, et al., (1999), Plasma waves observed during cusp energetic particle events and their correlation with Polar and Akebono satellite and ground data, Adv. Space. Res., 24, 23.

Sandahl, I, et al. (1997), Cusp and boundary layer observations by Interball, Adv. Space. Res. 20, 823.

Seki, K., R. C. Elphic, M. Hirahara, T. Terasawa, and T. Mukai (2001), On atmospheric loss of oxygen ions from earth through magnetospheric processes, Science, 291, 1939–1941.

Sharp, R. D., D. L. Carr, W. K. Peterson, and E. G. Shelley (1981), Ion Streams in the Magnetotail, *J. Geophys. Res.*, *86*(A6), 4639–4648, doi:10.1029/JA086iA06p04639.

Shelley, E.G., A.G. Ghielmetti, H. Balsiger, R.K. Black, J.A. Bowles, R.P. Bowman, O. Bratschi, J.L. Burch, C.W. Carlson, A.J. Coker, J.F. Drake, J. Fischer, J. Geiss, A. Johnstone, D.L. Kloza, O.W. Lennartsson, A.L. Magoncelli, G.. Pashmann, W.K. Peterson, H. Rosenbauer, T.C. Sanders, M. Steinacher, D.M. Walton, B.A. Whalen, and

D.T. Young (1995), The Toroidal Imaging Mass-Angle Spectrograph (TIMAS) for the Polar Mission, Space Science Reviews, 71, 497.

Strangeway, R. J., R. E. Ergun, Y.-J. Su, C. W. Carlson, and R. C. Elphic (2005), Factors controlling ionospheric outflows as observed at intermediate altitudes, J. Geophys. Res., 110, A03221, doi:10.1029/2004JA010829.

Trattner, K.J., S.A. Fuselier, W.K. Peterson, and S-W Chang (1999), Comment on: "Correlation of Cusp MeV Helium with Turbulent ULF Power Spectrum and its Implications", Geophys. Res. Lett, 26, 1361.

Trattner. K.J., S.A. Fuselier, W.K. Peterson, S.-W. Chang, R. Friedel, and M.R. Aellig (2001), Origins of Energetic Ions in the Cusp, *J. Geophys. Res., 106*, 5967-5976.

Trattner, K. J., J. S. Mulcock, S. M. Petrinec, and S. A. Fuselier (2007), Probing the boundary between antiparallel and component reconnection during southward interplanetary magnetic field conditions, J. Geophys. Res., 112, A08210, doi:10.1029/2007JA012270.

Trattner, K. J., S. M. Petrinec, S. A. Fuselier, W. K. Peterson, and R. Friedel (2010), Cusp energetic ions as tracers for particle transport into the magnetosphere, J. Geophys. Res., 115, A04219, doi:10.1029/2009JA014919.

Vogiatzis, I.I., T. E. Sarris, E. T. Sarris, O. Santol´ık, I. Dandouras, P. Robert, T. A. Fritz, Q.-G. Zong, and H. Zhang (2008), Cluster observations of particle acceleration up to supra-thermal energies in the cusp region related to low-frequency wave activity – possible implications for the substorm initiation process, Ann. Geophys., 26, 653–669.

Yau, A.W., W.K. Peterson, and E.G. Shelley (1988), Quantitative Parameterization of Energetic Ionospheric Ion Outflow, in Modeling Magnetospheric Plasma, Geophysical Monograph 44, American Geophysical Union, Washington, DC. 211.

Yau, A.W. and M. André (1997), Sources of ion outflow in the high latitude ionosphere, Space Sci. Rev., 80, 1-25.

Young, D. T., H. Balsiger, and J. Geiss (1982), Correlations of Magnetospheric Ion Composition With Geomagnetic and Solar Activity, *J. Geophys. Res.*, *87*(A11), 9077–9096, doi:10.1029/JA087iA11p09077.

Zhou, X. W., C. T. Russell, G. Le, S. A. Fuselier, and J. D. Scudder (2000), Solar wind control of the polar cusp at high altitude, *J. Geophys. Res.*, 105(A1), 245–251.